Banner appropriate to article type will appear here in typeset article

Numerical Simulation of Hypersonic Axisymmetric Base Flow

Yongkai Chen[1]†, Xuerui Mao[1]

[1]School of Interdisciplinary Science, Beijing Institute of Technology, Beijing 100081, PR China

(Received xx; revised xx; accepted xx)

XXXXXXXXXXXX

Key words: Authors should not enter keywords on the manuscript, as these must be chosen by the author during the online submission process and will then be added during the typesetting process (see Keyword PDF for the full list). Other classifications will be added at the same time.

---

1. Introduction

Investigations of the near-wake generated by a high-speed slender body have been studied over decades due to its importance to the areodynamic design. Most of the research focus on the

2. Problem formulation

2.1. *Flow set-up*

A sketch of the flow set-up is shown in figure 1. A slender cylinder of radius R has its axisymmetric axis aligned with the x-direction and the origin is located at the center of the cylinder base. Distances upstream and downstream of the base plane are $10R$ and $16R$, respectively. Such a choice gurantees a long enough distance for turbulence to develop along the cylinder, and the outflow boundary are far engough to affect the near-wake region. The far-field boundary is $10R$ from the axisymmetric axis. In total five cases are performed, with various Mach numbers and Reynolds numbers. The details of flow conditions are given in table 1. jfkd Riemann-invariant conditions are applied the far-field boundary. At the right boundary, the supersonic outflow condition is applied. All cases posses an isothermal no-slip wall conditions, with the wall temperature varied to keep a constant wall-to-recovery temperature ratio. For the inflow, a synthetic eddy method (SEM) is used to facilitate the development a turbulent boundary layer before it reaches the base corner. For a typical SEM, vortices of different length scales are generated in a virtual inlet domain, whose induced field are added to a prescribed mean flow profile to mimic the behaviour of a true turblent

† Email address for correspondence: JFMEditorial@cambridge.org

Abstract must not spill onto p.2

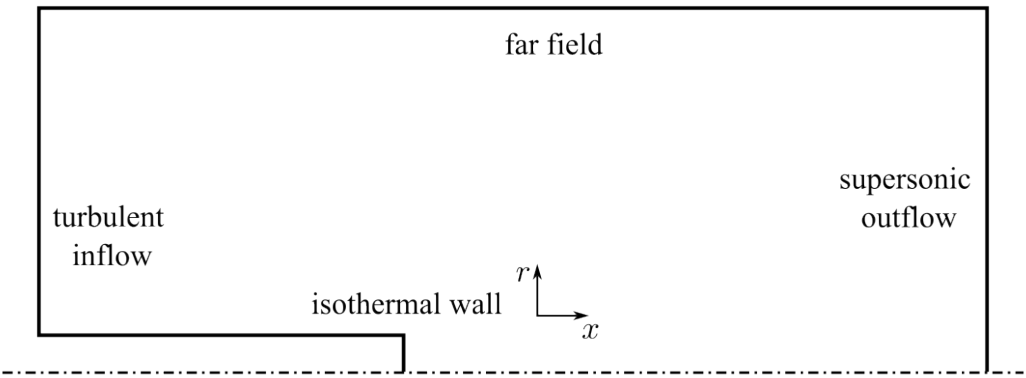

Figure 1: Sketch of the computational domain. Only an $x - r$ plane is presented for simplicity.

M_b	Re_m	Re_D	ρ_∞
6.4	$1e6$	$1e7$	?
6.4	$5.8e6$	$1e7$	?
6.4	$1e7$	$1e7$	?
7.7	$5.8e6$	$1e7$	?
9.0	$1e7$	$1e7$	?

Table 1: Freestream parameters of hypersonic baseflow simulations.

boudnary layer. A detailed review can be found in XXX and. In the current work, the inflow generation method is built upon the methodology proposed by **?**. Such method generate different shapes of vorticies based on the wall distance, and requires the viscous length and velocity scale *a priori*. In a high Mach nubmer compressible boundary layer, these scales often have strong variations with wall distance and are difficult to obtain with simple calculations. Here we generate mean flow profiles of velocity and temperature based on the method of **?**, which can then be used for the calculation of viscous length and velocity scales. With the above information, eddies of generatign. A more detailed discription can be found in Appendix XXX. In the current work, we limit the prescribed inlet Re_{δ_2} at 350 and a wall-to-recovery temperature ratio to 0.2.

2.2. *Governing equations*

The simulations are performed by solving the compressible Navier-Stokes equation, given as

$$\frac{\partial \rho}{\partial t} + \frac{\partial \rho u_j}{\partial x_j} = 0 \tag{2.1}$$

$$\frac{\partial \rho u_i}{\partial t} + \frac{\partial \rho u_i u_j}{\partial x_j} = -\frac{\partial p}{\partial x_i} + \frac{\partial \tau_{ij}}{\partial x_j} + \rho f_i \tag{2.2}$$

$$\frac{\partial \rho E}{\partial t} + \frac{\partial \rho u_j E}{\partial x_j} = -\frac{\partial p u_j}{\partial x_j} + \frac{\partial (u_k \tau_{kj} - q_j)}{\partial x_j} + \rho f_j u_j \tag{2.3}$$

Here τ_{ij} is the stress tensor given as

$$\tau_{ij} = (\mu + \mu_{\mathrm{sgs}}) \left(\frac{\partial u_i}{\partial x_j} + \frac{\partial u_j}{\partial x_i} - \frac{2}{3}\delta_{ij}\frac{u_k}{x_k} \right) \tag{2.4}$$

with subscript 'sgs' being the component contributed by sub-grid scale (SGS) model. The heat flux vector q_j is defined as

$$q_j = -C_p(\frac{\mu}{Pr} + \frac{\mu_{\mathrm{sgs}}}{Pr_{\mathrm{sgs}}})\frac{\partial T}{\partial x_j} \tag{2.5}$$

where C_p is the heat capacity at constant pressure, $\gamma = 1.4$ is the ratio of specific heat and $Pr = 0.72$ is the Prandtl number. At such high Mach number, there is a chance for the real-gas effectd to emerge, which is, however, beyong the scope of the current work. The fluid is assumed to be air and follow the ideal gas law, i.e., $p = \rho R_{\mathrm{gas}} T$. The gas constant R_{gas} takes the value of $286.9 J/(kg \cdot K)$. The dynamic viscosity is assumed to follow Sutherland's law **??**, which is

$$\mu = \frac{C_1 T^{3/2}}{T + S} \tag{2.6}$$

where $S = 110.4K$, $C_1 = 1.458 \times 10^{-6} kg/(m \cdot s \cdot \sqrt{K})$. Unless otherwise stated, the cylinder radius and free stream parameters are used for non-dimensionalization, i.e., R, ρ_∞, u_∞, T_∞.

2.3. *Numerical Setup*

(Yongkai: 1. We need to be careful about the code description here. 2. I prefer to rename the code (not COOLES), maybe Hyves.) The simulations are performed by a C++ code XXX, under development at the Data-Fluid Lab at Beijing Institute of Technology. The code is based on the flux reconstruction (FR) (Huynh 2007) method to provide a high-order, high flexibility solution for flow over complex geometries, and is designed for a hybrid CPU-GPU computational framework. The FR scheme approximates the solution with polynomials in each cell, and requires the evaluation of fluxes at the cell interface. In the current solver, a Rusanov Riemann sovler (Rusanov 1962) is used to calculate the inviscid flux. For the viscous flux, the local discontinuous Galerkin (LDG) (Cockburn & Shu 1998) method is used, with an upwind parameter of $\beta = 0.5$ and dissipation parameter of $\tau = 0.1$. For the time integration, a four-stage, third order strong stability preserving Runge-Kutta scheme (Gottlieb 2005) is adopted(Yongkai: make a double check). For all simulations, a polynomial order of $p = 4$ is used, corresponding to a 5th order of accuracy. The code is designed and tuned to the Sugon Z100 deep computing unit (DCU) to perform the large scale numerical simulations presented in this work. Parallelization of the code is achieved via the Message-Passing-Interface (MPI) on the CPU side. Several test cases including XXXXX are provided in the Appendix XXXX to justify the capability of the code to handle high-speed turbulent flow simulations.

3. Hypersonic Base Flow

3.1. *Incoming turbulent state*

here put figures:

1. The evolution of mean streamwise velocity along the x direction
2. Variation of the energy spectra. Maybe for all Mach

3.2. *Near-wake structures*

Mostly dynamics properties., fj

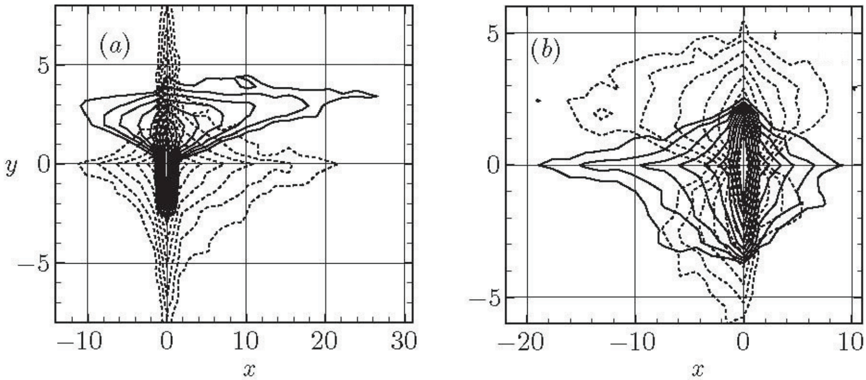

Figure 2: Trapped-mode wavenumbers, kd, plotted against a/d for three ellipses: ——, $b/a = 1$; $\cdots\cdots$, $b/a = 1.5$.

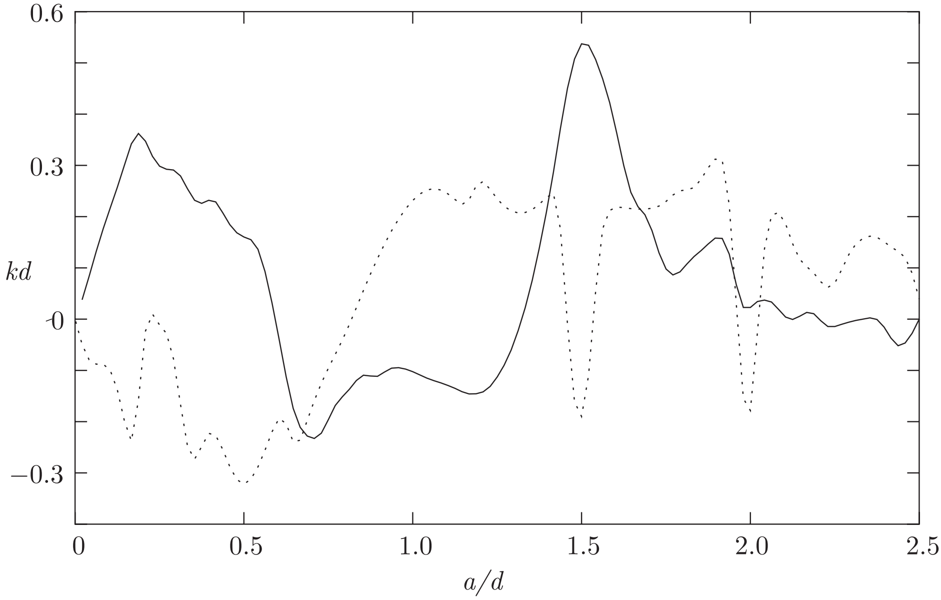

Figure 3: The features of the four possible modes corresponding to (*a*) periodic and (*b*) half-periodic solutions.

3.3. *Temperature Field and Wall heat flux*

Check the temperature distribution Q: 1. Time scale of this temperature evolution? 2. The heat flux at several locations: base, side

4. Figures and Tables

4.1. *Figures*

Each figure should be accompanied by a single caption, to appear beneath, and must be cited in the text. Figures should appear in the order in which they are first mentioned in the text. For example see figures 2 and 3.

Focus on Fluids articles must not exceed this page length

M_∞	Re_∞	ρ_∞ *et al.*	
6.4	5.8×10^6		0.042
0.55	1.39128	1.391	1.39131
0.7	1.32281	10.322	1.32288
0.913	1.34479	100.351	1.35185

Table 2: Values of kd at which trapped modes occur when $\rho(\theta) = a$.

4.2. *Tables*

Tables, however small, must be numbered sequentially in the order in which they are mentioned in the text. Words *table 1, table 2* should be lower case throughout. See table 2 for an example.

This is an example of dummy text. This is an example of dummy text.

5. Notation and style

Generally any queries concerning notation and journal style can be answered by viewing recent pages in the Journal. However, the following guide provides the key points to note. It is expected that Journal style and mathematical notation will be followed, and authors should take care to define all variables or entities upon first use. Also note that footnotes are not normally accepted. Abbreviations must be defined at first use, glossaries or lists/tables of abbreviations are not permitted.

5.1. *Mathematical notation*

5.1.1. *Setting variables, functions, vectors, matrices etc*

- **Italic font** should be used for denoting variables, with multiple-letter symbols avoided except in the case of dimensionless numbers such as Re, Pr and Pe (Reynolds, Prandtl, and Péclet numbers respectively, which are defined as `\Rey`, `\Pran` and `\Pen` in the template).

- **Upright Roman font** (or upright Greek where appropriate) should be used for:

  (i) (vI) label, e.g. T. t (transpose)

  (ii) Fixed operators: sin, log, d, Δ, exp etc.

  (iii) Constants: i ($\sqrt{-1}$), π (defined as `\upi`),e etc.

  (iv) Special Functions: Ai, Bi (Airy functions, defined as `\Ai` and `\Bi`), Re (real part, defined as `\Real`), Im (imaginary part, defined as `\Imag`), etc.

  (v) Physical units: cm, s, etc.

  (vi) Abbreviations: c.c. (complex conjugate), h.o.t. (higher-order terms), DNS, etc.

- **Bold italic font** (or bold sloping Greek) should be used for vectors (with the centred dot for a scalar product also in bold): $\boldsymbol{i} \boldsymbol{\cdot} \boldsymbol{j}$

- **Bold sloping sans serif font**, defined by the `\mathsfbi` macro, should be used for tensors and matrices: $\boldsymbol{\mathsf{D}}$

- **Calligraphic font** (for example $\mathcal{G}$, $\mathcal{R}$) can be used as an alternative to italic when the same letter denotes a different quantity use `\mathcal` in LaTeX)

5.1.2. *Other symbols*

Large numbers that are not scientific powers should not include commas, but should use a non-breaking space, and use the form 1600 or 16 000 or 160 000. Use O to denote 'of the order of', not the LaTeX $\mathcal{O}$.

The product symbol ($\times$) should only be used to denote multiplication where an equation is broken over more than one line, to denote a cross product, or between numbers . The $\boldsymbol{\cdot}$ symbol should not be used, except to denote a scalar product of vectors specifically.

5.1.3. *Example Equations*

This section contains sample equations in the JFM style. Please refer to the LaTeX source file for examples of how to display such equations in your manuscript.

$$(\nabla^2 + k^2)G_s = (\nabla^2 + k^2)G_a = 0 \tag{5.1}$$

$$\boldsymbol{\nabla} \boldsymbol{\cdot} \boldsymbol{v} = 0, \quad \nabla^2 P = \boldsymbol{\nabla} \boldsymbol{\cdot} (\boldsymbol{v} \times \boldsymbol{w}). \tag{5.2}$$

$$G_s, G_a \sim 1/(2\pi) \ln r \quad \text{as} \quad r \equiv |P - Q| \rightarrow 0, \tag{5.3}$$

$$\left.\begin{aligned}\frac{\partial G_s}{\partial y} = 0 \quad \text{on} \quad y = 0,\\ G_a = 0 \quad \text{on} \quad y = 0,\end{aligned}\right\} \tag{5.4}$$

$$-\frac{1}{2\pi}\int_0^\infty \gamma^{-1}[exp(-k\gamma|y-\eta|)+exp(-k\gamma(2d-y-\eta))]\cos k(x-\xi)t\mathrm{d}t, \qquad 0 < y, \quad \eta < d, \tag{5.5}$$

$$\gamma(t) = \begin{cases} -\mathrm{i}(1-t^2)^{1/2}, & t \leqslant 1\\ (t^2-1)^{1/2}, & t > 1. \end{cases} \tag{5.6}$$

$$-\frac{1}{2\pi}\int_0^\infty B(t)\frac{\cosh k\gamma(d-y)}{\gamma\sinh k\gamma d}\cos k(x-\xi)t\,\mathrm{d}t$$

$$G = -\frac{1}{4}\mathrm{i}(H_0(kr)+H_0(kr_1)) - \frac{1}{\pi}\int_0^\infty \frac{\mathrm{e}^{-k\gamma d}}{\gamma\sinh k\gamma d}\cosh k\gamma(d-y)\cosh k\gamma(d-\eta) \tag{5.7}$$

Note that when equations are included in definitions, it may be suitable to render them in line, rather than in the equation environment: $\boldsymbol{n}_q = (-y'(\theta), x'(\theta))/w(\theta)$. Now $G_a = \frac{1}{4}Y_0(kr) + \widetilde{G_a}$ where $r = \{[x(\theta)-x(\psi)]^2 + [y(\theta)-y(\psi)]^2\}^{1/2}$ and $\widetilde{G_a}$ is regular as $kr \to 0$. However, any fractions displayed like this, other than $\frac{1}{2}$ or $\frac{1}{4}$, must be written on the line, and not stacked (ie 1/3).

$$\begin{aligned}\frac{\partial}{\partial n_q}\left(\frac{1}{4}Y_0(kr)\right) &\sim \frac{1}{4\pi w^3(\theta)}[x''(\theta)y'(\theta) - y''(\theta)x'(\theta)]\\ &= \frac{1}{4\pi w^3(\theta)}[\rho'(\theta)\rho''(\theta) - \rho^2(\theta) - 2\rho'^2(\theta)] \quad \text{as} \quad kr \to 0. \end{aligned} \tag{5.8}$$

$$\frac{1}{2}\phi_i = \frac{\pi}{M}\sum_{j=1}^{M}\phi_j K_{ij}^a w_j, \qquad i = 1, \ldots, M, \tag{5.9}$$

where

$$K_{ij}^a = \begin{cases} \partial G_a(\theta_i, \theta_j)/\partial n_q, & i \neq j\\ \partial \widetilde{G_a}(\theta_i, \theta_i)/\partial n_q + [\rho_i'\rho_i'' - \rho_i^2 - 2\rho_i'^2]/4\pi w_i^3, & i = j. \end{cases} \tag{5.10}$$

$$\rho_l = \lim_{\zeta \to Z_l^-(x)} \rho(x,\zeta), \quad \rho_u = \lim_{\zeta \to Z_u^+(x)} \rho(x,\zeta) \tag{5.11a,b}$$

$$(\rho(x,\zeta), \phi_{\zeta\zeta}(x,\zeta)) = (\rho_0, N_0)j \quad \text{for} \quad Z_l(x) < \zeta < Z_u(x). \tag{5.12}$$

$$\tau_{ij} = (\overline{\overline{u}_i\overline{u}_j} - \overline{u}_i\overline{u}_j) + (\overline{\overline{u}_i u_j^{SGS} + u_i^{SGS}\overline{u}_j}) + \overline{u_i^{SGS}u_j^{SGS}}, \tag{5.13a}$$

$$\tau_j^\theta = (\overline{\overline{u}_j\overline{\theta}} - \overline{u}_j\overline{\theta}) + (\overline{\overline{u}_j\theta^{SGS} + u_j^{SGS}\overline{\theta}}) + \overline{u_j^{SGS}\theta^{SGS}}. \tag{5.13b}$$

$$\boldsymbol{Q}_C = \begin{bmatrix} -\omega^{-2}V_w' & -(\alpha^t\omega)^{-1} & 0 & 0 & 0 \\ \dfrac{\beta}{\alpha\omega^2}V_w' & 0 & 0 & 0 & \mathrm{i}\omega^{-1} \\ \mathrm{i}\omega^{-1} & 0 & 0 & 0 & 0 \\ \mathrm{i}R_\delta^{-1}(\alpha^t + \omega^{-1}V_w'') & 0 & -(\mathrm{i}\alpha^t R_\delta)^{-1} & 0 & 0 \\ \dfrac{\mathrm{i}\beta}{\alpha\omega}R_\delta^{-1}V_w'' & 0 & 0 & 0 & 0 \\ (\mathrm{i}\alpha^t)^{-1}V_w' & (3R_\delta^{-1} + c^t(\mathrm{i}\alpha^t)^{-1}) & 0 & -(\alpha^t)^{-2}R_\delta^{-1} & 0 \end{bmatrix}. \tag{5.14}$$

$$\boldsymbol{\eta}^t = \hat{\boldsymbol{\eta}}^t \exp[\mathrm{i}(\alpha^t x_1^t - \omega t)], \tag{5.15}$$

where $\hat{\boldsymbol{\eta}}^t = \boldsymbol{b}\exp(\mathrm{i}\gamma x_3^t)$.

$$\mathrm{Det}[\rho\omega^2\delta_{ps} - C_{pqrs}^t k_q^t k_r^t] = 0, \tag{5.16}$$

$$\langle k_1^t, k_2^t, k_3^t\rangle = \langle \alpha^t, 0, \gamma\rangle \tag{5.17}$$

$$\boldsymbol{f}(\theta,\psi) = (g(\psi)\cos\theta, g(\psi)\sin\theta, f(\psi)). \tag{5.18}$$

$$f(\psi_1) = \frac{3b}{\pi[2(a+b\cos\psi_1)]^{3/2}}\int_0^{2\pi}\frac{(\sin\psi_1 - \sin\psi)(a+b\cos\psi)^{1/2}}{[1-\cos(\psi_1-\psi)](2+\alpha)^{1/2}}\mathrm{d}x, \tag{5.19}$$

$$\begin{aligned} g(\psi_1) = {} & \frac{3}{\pi[2(a+b\cos\psi_1)]^{3/2}}\int_0^{2\pi}\left(\frac{a+b\cos\psi}{2+\alpha}\right)^{1/2}\left\{f(\psi)[(\cos\psi_1 - b\beta_1)S + \beta_1 P]\right. \\ & \times\frac{\sin\psi_1-\sin\psi}{1-\cos(\psi_1-\psi)} + g(\psi)\left[\left(2+\alpha-\frac{(\sin\psi_1-\sin\psi)^2}{1-\cos(\psi-\psi_1)} - b^2\gamma\right)S\right. \\ & \left.\left. + \left(b^2\cos\psi_1\gamma - \frac{a}{b}\alpha\right)F(\frac{1}{2}\pi,\delta) - (2+\alpha)\cos\psi_1 E(\frac{1}{2}\pi,\delta)\right]\right\}\mathrm{d}\psi, \end{aligned} \tag{5.20}$$

$$\alpha = \alpha(\psi,\psi_1) = \frac{b^2[1-\cos(\psi-\psi_1)]}{(a+b\cos\psi)(a+b\cos\psi_1)}, \quad \beta - \beta(\psi,\psi_1) = \frac{1-\cos(\psi-\psi_1)}{a+b\cos\psi}. \tag{5.21}$$

$$\left.\begin{aligned} H(0) = \frac{\epsilon\overline{C}_v}{\tilde{v}_T^{1/2}(1-\beta)}, \quad & H'(0) = -1 + \epsilon^{2/3}\overline{C}_u + \epsilon\hat{C}_u'; \\ H''(0) = \frac{\epsilon u_*^2}{\tilde{v}_T^{1/2}u_P^2}, \quad & H'(\infty) = 0. \end{aligned}\right\} \tag{5.22}$$

LEMMA 1. *Let $f(z)$ be a trial* **?**, *pp. 231–232 function defined on* $[0,1]$. *Let* Λ_1 *denote the ground-state eigenvalue for* $-\mathrm{d}^2g/\mathrm{d}z^2 = \Lambda g$, *where* g *must satisfy* $\pm\mathrm{d}g/\mathrm{d}z + \alpha g = 0$ *at*

$z = 0, 1$ *for some non-negative constant* α. *Then for any* f *that is not identically zero we have*

$$\frac{\alpha(f^2(0) + f^2(1)) + \displaystyle\int_0^1 \left(\frac{\mathrm{d}f}{\mathrm{d}z}\right)^2 \mathrm{d}z}{\displaystyle\int_0^1 f^2 \mathrm{d}z} \geqslant \Lambda_1 \geqslant \left(\frac{-\alpha + (\alpha^2 + 8\pi^2\alpha)^{1/2}}{4\pi}\right)^2. \tag{5.23}$$

Corollary 1. *Any non-zero trial function* f *which satisfies the boundary condition* $f(0) = f(1) = 0$ *always satisfies*

$$\int_0^1 \left(\frac{\mathrm{d}f}{\mathrm{d}z}\right)^2 \mathrm{d}z. \tag{5.24}$$

6. Citations and references

All papers included in the References section must be cited in the article, and vice versa. Citations should be included as, for example "It has been shown (**?**) that..." (using the `\citep` command, part of the natbib package) "recent work by **?**..." (using `\citet`). The natbib package can be used to generate citation variations, as shown below.

`\citet[pp. 2-4]{Hwang70}`:

?, pp. 2-4

`\citep[p. 6]{Worster92}`:

(**?**, p. 6)

`\citep[see][]{Koch83, Lee71, Linton92}`:

(see **???**)

`\citep[see][p. 18]{Martin80}`:

(see **?**, p. 18)

`\citep{Brownell04,Brownell07,Ursell50,Wijngaarden68,Miller91}`:

(**?????**)

(**?**)

?

(**?**)

The References section can either be built from individual `\bibitem` commands, or can be built using BibTex. The BibTex files used to generate the references in this document can be found in the JFM LaTeX template files folder provided on the website here.

Where there are up to ten authors, all authors' names should be given in the reference list. Where there are more than ten authors, only the first name should appear, followed by *et al.*

Supplementary data. Supplementary material and movies are available at
https://doi.org/10.1017/jfm.2019...

Acknowledgements. The authors would like to thank the technical support from the on the code-adpation and tuning on DCU and the computational resource[SOGON zhisuan]. XXXX..... / CHINA postdoctoral

Funding. Please provide details of the sources of financial support for all authors, including grant numbers. Where no specific funding has been provided for research, please provide the following statement: "This research received no specific grant from any funding agency, commercial or not-for-profit sectors."

Declaration of interests. The authors report no conflict of interest.

Data availability statement. The data that support the findings of this study are openly available in [repository name] at http://doi.org/[doi], reference number [reference number]. See JFM's research transparency policy for more information

Author ORCIDs. Authors may include the ORCID identifers as follows. F. Smith, https://orcid.org/0000-0001-2345-6789; B. Jones, https://orcid.org/0000-0009-8765-4321

Author contributions. Authors may include details of the contributions made by each author to the manuscript'

Appendix A.

In this section, X test cases were provided to validate the solver.

A.1. *Sod's shock tube problem? or maybe*

inviscid

A.2. *Viscous shock tube*

2D - viscous

A.3. *Turbulent channel flow*

A compressible turbulent channel flow at $M_b = 1.5, Re_b = 5000$ is test in this subsection. The simulation is performed at $p = 4$, with a number of cells of $N_x \times N_y \times N_z = X \times X \times X$, leading to a total DoF of XXX. Mean flow statistics are compared with the DNS data by Chen & Scalo (2021), as shown in figure XX and XX. Both the mean streamwise velocity profile and the Reynolds stresses show good agreement with the reference data.

REFERENCES

Chen, Yongkai & Scalo, Carlo 2021 Trapped waves in supersonic and hypersonic turbulent channel flow over porous walls. *Journal of Fluid Mechanics* **920**, A24.

Cockburn, Bernardo & Shu, Chi-Wang 1998 The local discontinuous galerkin method for time-dependent convection-diffusion systems. *SIAM journal on numerical analysis* **35** (6), 2440–2463.

Gottlieb, Sigal 2005 On high order strong stability preserving runge-kutta and multi step time discretizations. *Journal of Scientific Computing* **25**, 105–128.

Huynh, Hung T 2007 A flux reconstruction approach to high-order schemes including discontinuous galerkin methods. In *18th AIAA computational fluid dynamics conference*, p. 4079.

Rusanov, Vladimir Vasil'evich 1962 The calculation of the interaction of non-stationary shock waves and obstacles. *USSR Computational Mathematics and Mathematical Physics* **1** (2), 304–320.